

The role of fluids in the chemical composition of the upper holocene sediment layer in the russian sector of the South-East Baltic

Alexander Krek¹, Viktor Krechik¹, Aleksandr Danchenkov^{1,2}, and Galina Mikhnevich²

Received 26 February 2020; accepted 9 April 2020; published 5 November 2020.

An analysis of the of the chemical composition of the upper slimy precipitate layer in the Gdansk Deep demonstrated increased concentrations of Ca, Mg, K, and Na in areas associated with tectonic faults. A cluster analysis of sediment layers, with a resolution of 1 cm, revealed an alternation of layers in the pockmark with a shortening of cluster bonds between the marker elements, indicating that the groundwater enters the sedimentary strata. **KEYWORDS:** South-East Baltic; bottom sediments; cluster analysis; groundwater.

Citation: Krek, Alexander, Viktor Krechik, Aleksandr Danchenkov, and Galina Mikhnevich (2020), The role of fluids in the chemical composition of the upper holocene sediment layer in the russian sector of the South-East Baltic, *Russ. J. Earth. Sci.*, 20, ES6006, doi:10.2205/2020ES000719.

Introduction

Sedimentogenesis in semi-closed tideless basins is characterized by a high terrigenous component and involves the accumulation and further transformation of sediment. The mechanism of bottom sediment accumulation in the Gdansk Deep has been studied thoroughly, and it is primarily associated with the gravitational sedimentation of suspended matter [Emelyanov, 1986, 2002, 2017; Pempkowiak *et al.*, 1999; Roussiez *et al.*, 2005; Rubio *et al.*, 2000]. The transformation of sedimentary matter is controlled by abiotic and biotic factors, as well as by a number of features of the thermohaline structure of the Baltic Sea and its water circulation [Bulczak *et al.*, 2016; Lund-Hansen and Skyum, 1992].

¹Shirshov Institute of Oceanology RAS, Moscow, Russia

²Immanuel Kant Baltic Federal University, Kaliningrad, Russia

Contemporary research most often seeks to study these two processes. However, in addition to external factors, there exist mechanisms for the transformation of sedimentary matter that are associated with activity from the subsurface (for example, streams of fluids – groundwater, gases). Submarine groundwater discharge has long been recognized as an important source of fresh water and various chemicals such as trace elements, biogenes, and organic and inorganic carbon [Burnett *et al.*, 2006; Charette *et al.*, 2001; Moore, 2010; Oberdorfer *et al.*, 1990; Slomp and Van Cappellen, 2004]. Meanwhile, the role of groundwater in the formation of bottom sediment is most often not considered. Although discharge volume may be relatively small, especially in the areas of large rivers, groundwater plays an important role in the global water cycle. Moreover, since groundwater is most often enriched with chemical elements not characteristic of sea water composition, in some areas, their interaction with bottom sediment may form a unique ecosystem and become an important component of its activity [Szymczycha *et al.*, 2012, 2014, 2016]. Thus, the study of the effect of submarine groundwater discharge on the sedimentation process is the issue to be studied in this project.

Study Area

The Baltic Sea Basin and, in particular, the Gdansk Deep, is the final drainage element of the underground reservoir system located to the south and southeast of the Baltic coast. The deep-sea basins, isolated by permanent pycnocline, have specific sedimentation conditions, primarily due to the peculiarities of benthic circulation. This leads to the formation of a slimy precipitation area in the Gdansk Deep at a depth of more than 70 m. Quasi-stable hydrochemical conditions in the bottom layer are occasionally violated during periods of advection of the North Sea waters (MBI), which cause the reductive-oxidative conditions to change and the velocities of bottom currents to increase significantly [Bulczak et al., 2016; Mohrholz et al., 2015].

Along with a thick mass of Holocene silts [Emelyanov, 1998] overlapping the fault areas, features of the hydrological regime create favorable conditions for the formation and existence of gas-saturated sediments and landforms such as pockmarks (Figure 1). Pockmark systems indicate fluid influx from sedimentary strata into the water. Gas-saturated sediments and flows of methane and its homologs in the southeastern part of the Baltic Sea have been well studied [Ulyanova et al., 2012]. In such areas, there is a high probability of groundwater coming to the surface or penetrating into the sedimentary mass.

Geological Environment of the Area

According to [Petrov, 2010], a system of faults, primarily dating from the Devonian Period, associated with the formation of the Baltic syncline, can be distinguished in the sedimentary sheath of the Russian sector of the southeastern part of the Baltic Sea. Some of these faults affect the sedimentary mass down to the quaternary deposits [Earth Physics Institute, 2008; Petrov, 2010]. Such fault areas demonstrate a link between different underground reservoirs [Triponis, 1973]. Land anomalies in the magnitude of groundwater mineralization are frequently noted; among them, in particular, are the Upper Cretaceous and intermorainic Pleistocene underground reservoirs resulting from the flow of water from underlying underground reservoirs due to discontinuous faults [Zagorodnykh,

2011]. It is expected that a similar process occurs in the water area.

Acoustic anomalies (as well as pockmarks), usually confined to paleocuts and fault areas indicating the flow of deep gases (fluids) through a permeable sedimentary sheath, are frequently found in the study area [Blazhchishin, 1998; Sviridov, 1990; Sviridov and Yemelyanov, 2000]. This is facilitated by the fractured structure of the underlying Lower Holocene and Upper Pleistocene rocks [Blazhchishin, 1998]. Groundwater may flow in conjunction with gas from the sedimentary strata.

Columns 37056 and 37057 are located in the acoustic anomaly area (see Figure 1 in the inset), confined to the valley and lake cuts that coincide with the extension of the fault, which is connected to the structural Upper Cretaceous ledge. The roots of the anomalies extend to the underlying Triassic/Jurassic stratum, which contains feeders that often end in Holocene deposits [Blazhchishin, 1998].

A combination of several key factors, such as active faults, the feathering-out of Cretaceous deposits, structural ledges and cuts, and the fracturing of the Late Pleistocene and Lower Holocene deposits may contribute to the discharge of groundwater in the area investigated.

Groundwater Composition

Groundwater in the area of the acoustic anomaly may be represented by Jurassic underground reservoirs, as per the map of pre-Quaternary deposits [Petrov, 2010]. The Oxford-Tithonian underground reservoir is limited to the upper part of the Jurassic section. The waters are brackish and are classified as being of the sodium chloride type, and their mineralization varies from 12 to 17 g/dm³ (Table 1) [Grigyalis and Kondratas, 1983; Nikutina, 2011; Sidorenko, 1970].

Materials and Methods

The significant thickness of silt sediments and the blurred water-bottom interface present major difficulties in the detection of salinity inversions. Firstly, the fluid influx is scattered in the silt mass and is mixed with seawater in sediments, and, secondly, silt suspension does not allow for reliable

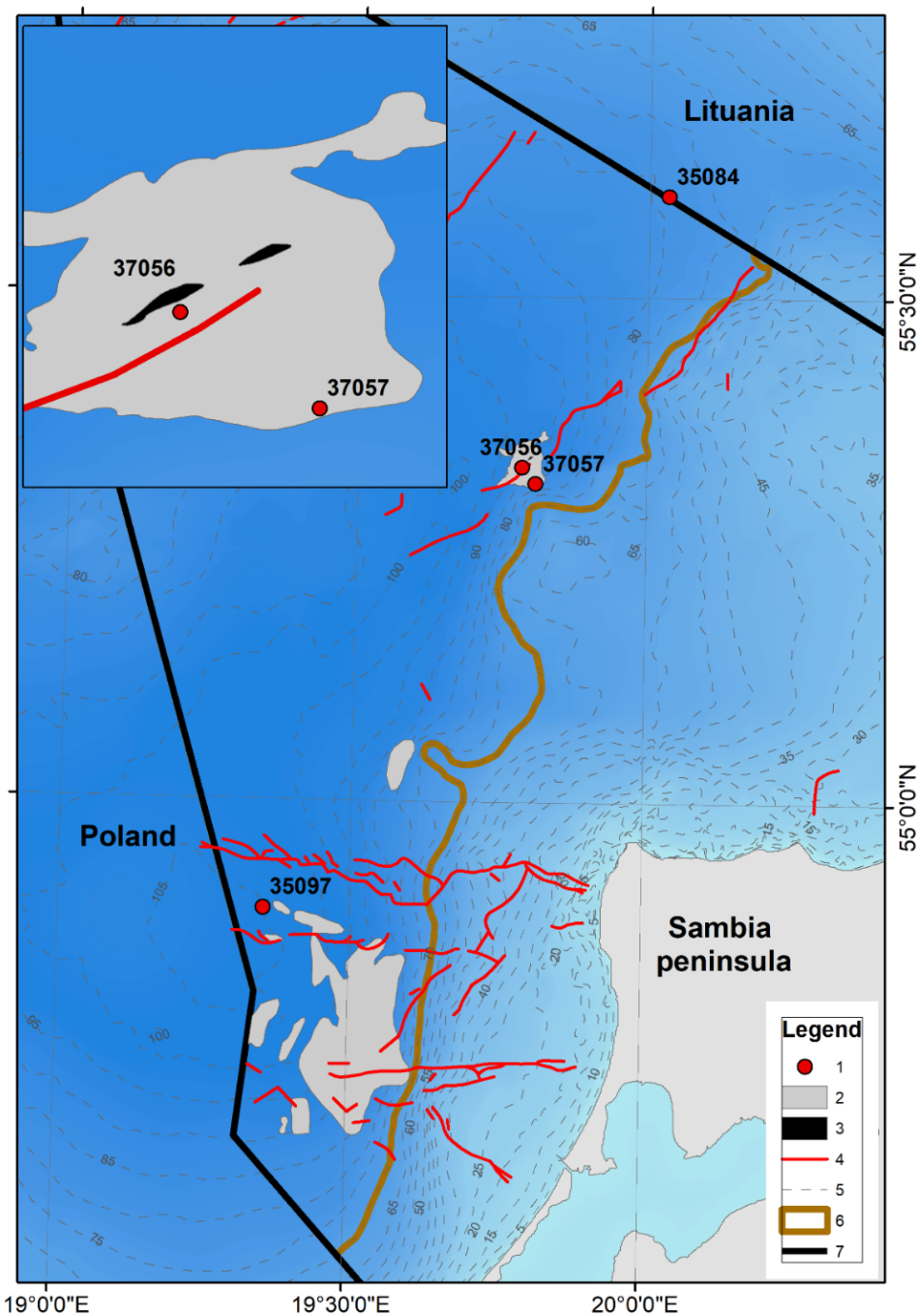


Figure 1. Study area. Legend: 1 – Sampling points; 2 – Gas-saturated sediments; 3 – Pockmarks; 4 – Fault areas, as per [*Otmas et al., 2006*]; 5 – Isobaths, m; 6 – Boundary of silt distribution in the Gdansk Deep; 7 – EEZ Russia.

Table 1. Content of Basic Ions in Sea Water and Groundwater

Ions	Ion content in sea water, mg/l	Ion content in the groundwater of the Upper Jurassic deposits, mg/l [<i>Grigyalis and Kondratas, 1983</i>]
Na ⁺	2261.25	4492.9
K ⁺	81.75	4492.9
Ca ²⁺	108.00	569.2
Mg ²⁺	284.25	266.1

Table 2. Laboratory Calibration Values for Chemical Elements

	Sample composition, %						Sample composition, ppm								
	Fe	Mn	K	Na	Ca	Mg	Ti	Cu	Zn	Co	Ni	Cr	Cd	Pb	As
Values obtained on standard samples	4.39	0.30	1.50	1.18	1.39	1.00	0.27	54	92	16	57	62	0.2	19	20
Certified reference values	4.90±0.30±0.54	1.83±0.05	1.45±0.36	1.32±0.28	1.20±0.23	0.21	0.25±0.05	52±7	96±14	18±2	54±6	66±4	0.2±0.03	21±3	18±3

probe measurement directly at solid boundaries, where the probe sensors are silted and display values which are known to be incorrect.

Therefore, a method based on changes in the geochemical composition of the upper sediment layer was used to identify the potential characteristics of groundwater discharge. We used data on the content of chemical elements in four columns with different positions relative to the fault areas and pockmarks. Column 37056 is located in close proximity to the fault and pockmark, Column 37057 is located in the peripheral area of gas-saturated sediments, and no pockmarks or faults are identified in the area of Columns 35084 and 35097 – they make up the “background.”

Sampling

Columns of bottom sediments were sampled by sealed geological tube using the Lauri-Niemisto system on the 35th and 37th voyages of the R/V *Akademik Nikolai Strakhov* (see Figure 1). After the tube was lifted back to the deck, the column was broken down with a resolution of 1 cm. Column 35084 was 56 cm, Column 35097 was 51 cm, Column 37056 was 81 cm, and Column 37057 was 76 cm. Samples were taken with an inert sampler and packaged in plastic bags. They were stored in a ship refrigerator at a temperature of +4°C, and were delivered to the coastal laboratory and analyzed within a week.

Laboratory Tests

The content of the elements in the soil samples studied was determined by atomic absorption analysis in the laboratory of the P. P. Shirshov Institute

of Oceanology – Atlantic Branch, using the method of quantitative chemical analysis of the Federal Scientific and Methodological Center for Laboratory Research and Certification of Mineral Raw Materials of the N. M. Fedorovsky All-Russian Scientific-Research Institute of Mineral Resources No. 450-C, as well as the VIMS instructions on chemical spectral analysis methods No. 155-XC.

The decomposition of samples was carried out using the method described in [*Khandros and Shaidurov, 1980*].

Cadmium and lead were determined using the Kvant-2 ETA atomic absorption spectrometer with electrothermal atomization, and the remaining elements were determined using the Varian AA240FS flame atomic absorption spectrometer.

A test charge of the sample (0.25 g) in a platinum crucible was placed in a muffle furnace and heated to a temperature of 500°C. Then, 5 ml of hydrofluoric acid and 1 ml of perchloric acid were added to the ash residue and dried completely. 5 ml of hydrochloric acid was poured onto the dry residue and heated until the salts were completely dissolved. The resulting solution was transferred into a 50 cm³ volumetric flask, brought to the mark with water, and stirred. Next, the concentration of elements in the resulting solutions was determined using atomic absorption spectrometers by measuring their atomic absorption (optical density of atomic vapor), using graduations for solutions with known concentrations of the elements identified. To control the accuracy of the analysis, parallel samples of the studied samples were also used, as well as a standard soil sample with a known concentration of the determined elements.

All results of instrumental measurements were subject to verification with reference indicators to identify possible errors. Determination limits and the range of error are displayed in Table 2.

Statistics

A hierarchical cluster (HC) analysis was used to investigate the similarities between concentrations of all 15 chemical elements from the sediment samples layers. The HC analysis was performed in two steps. At the first stage, all distributions of concentrations for each tube of sediment were examined to divide the sample into similar groups. At the second stage, linkages between the chemical elements inside each group identified at the first stage were analyzed.

Before performing the HC, the distributions of the chemical element concentrations were standardized both for each tube sample at the first stage and for each group at the second stage. The standardization procedure consisted of transforming the distribution data by subtracting the distribution mean value from each value and dividing it by the standard deviation. Thus, the variables were standardized as:

$$V_{sti} = \frac{V_i - V_{\text{mean}}}{\sigma(V)}$$

where V_{sti} represents the standardized variable, V_i is the measured value, V_{mean} is the total distribution mean and $\sigma(V)$ is the standard deviation of the distribution.

In this study, the HC analysis was performed using Ward's method as the amalgamation rule. This method uses an analysis of variance to evaluate the distances between clusters. See [Ward, 1963] for details. Euclidean distance was used as the geometric distance between different clusters in the multidimensional space. It is computed as: Distance $(x, y) = \sqrt{\sum_i (x_i - y_i)^2}$.

Descriptive statistics for both sample tubes and for each group inside them were also calculated. Microsoft Excel 2007 and SPSS 10 (Statistical Package for the Social Sciences) software was used to perform the statistical analyses.

Results

Description of Bottom Sediment Columns

Column 35084

- 0–1 cm: homogeneous loose olive silts (5Y 5/4) with black silt deposit (5Y 2.5/1);
- 1–2 cm: layered silt of olive (5Y 5/4) and light grey color (5Y 7/1);
- 2–4 cm: dark olive-grey silts (5Y 3/2);
- 5–41 cm: homogeneous silts with a smooth color change from (5Y 4/1) to (5Y 3/1);
- 12–13 cm: a transversal border of olive-grey (5Y 4/2) silt intersects with dark grey silts (5Y 4/1);
- 42–49 cm: silts of olive-grey color brighten gradually with depth (from 5Y 4/2 to 5Y 5/2);
- 49–56 cm: dense silts of grey-blue color (GLEY 2 6/10B).

Column 35097

- 0–26 cm: loose black aleurite-pelitic silts, on which an olive-grey (5Y 4/2);
- 2–3 mm silt deposit was observed;
- 26–51 cm: density of deposits increases, content of the silt fraction decreases, color changes to uniform grey (5Y 5/1).

Column 37056

- 0–9 cm: loose hydric silts of dark yellow-brown (10YR 3/4) color, yellow-brown color on the surface (10YR 4/5);
- 10–23 cm: grey (10YR 3/1) silts with black (10YR 2/1) inclusions;
- 23–61 cm: homogeneous dark grey silts (10YR 3/1-4/1);
- 62–81 cm: homogeneous black silts.

Column 37057

- 0–1 cm: liquefied aleurite-pelitic silts of dark yellow-brown (10YR 4/4) color;
- 1–6 cm: dark grey-brown (10YR 3/4-4/4) loose silts;
- 7–18 cm: black inclusions are observed in dark grey-brown (10YR 3/4-4/4) aleurite-pelitic silts (10YR 2/1);
- 18–56 cm: sediments are composed of homogeneous dark grey (10YR 3/1-4 / 1) aleurite-pelitic silts, which gradually brighten to grey shades by 71 cm (10YR 4/1-5/1).

Table 3. Averaged Content of Chemical Elements in Columns of Bottom Sediments of the Russian Sector of the South-East Baltic Sea

	Fe	Mn	K	Na	Ca	Mg	Elements									
							%	Ti	Cu	Zn	Co	Ni	Cr	Cd	Pb	As
0–56 cm														35084		
Min	3.74	0.01	1.05	0.73	0.58	0.4		0.2	34	66	6	30	74	0.1	14	10
Max	5.93	0.04	2.84	2.80	1.36	1.3		0.3	80	185	20	69	160	0.7	68	27
Mean	4.67	0.02	1.67	1.25	0.90	0.7		0.3	47	111	12	46	113	0.2	36	16
Sigma	0.55	0.01	0.30	0.41	0.19	0.2		0.0	9	29	3	9	17	0.2	14	3
0–51 cm														35097		
Min	3.50	0.03	1.21	1.00	0.71	0.6		0.2	36	80	13	36	85	0.1	17	16
Max	5.78	0.14	2.40	2.55	2.12	1.3		0.4	70	189	23	69	163	0.7	86	30
Mean	4.83	0.07	1.64	1.65	1.05	0.8		0.3	47	124	18	53	129	0.3	50	24
Sigma	0.46	0.03	0.26	0.43	0.22	0.2		0.0	8	28	2	8	17	0.2	22	3
0–81 cm														37056		
Min	3.58	0.01	1.54	1.21	1.00	0.9		0.3	38	81	7	34	78	0.1	14	10
Max	6.36	0.06	3.13	4.82	3.02	1.6		0.4	86	153	27	55	121	0.7	91	68
Mean	4.81	0.02	2.03	1.91	1.48	1.2		0.3	46	113	13	42	97	0.2	36	23
Sigma	0.78	0.01	0.32	0.54	0.44	0.2		0.0	9	20	4	5	8	0.2	17	7
0–76 cm														37057		
Min	3.44	0.01	1.43	1.00	0.80	0.7		0.2	30	77	9	36	70	0.1	7	13
Max	6.17	0.10	3.18	3.39	2.71	1.7		0.4	65	146	23	72	135	0.4	40	30
Mean	4.54	0.05	1.95	1.65	1.37	1.0		0.3	41	103	14	49	100	0.2	22	22
Sigma	0.71	0.02	0.27	0.55	0.50	0.2		0.1	6	15	3	9	14	0.1	6	4

Results of Chemical Analysis

On average, the content of the principal macroelements (K, Na, Ca, Mg) in the fault area was higher than in the background areas. Thus, in Columns 37056 and 37057, the K content was 20% higher than in Columns 35084 and 35097. Na was 23%, and Ca and Mg were 46% (Table 3). Moreover, the Fe content (normalizing element, as per *Uścinowicz et al.* [2011]) was similar. On average, it differed by 2%, which falls within the error limit of the determination method. Conversely, Cu, Zn, Co, Ni, Cr, Cd, Pb showed negative dynamics in the fault area, which may be due to their removal from the sediment under the influence of biological processes, or leaching by the groundwater, which is undersaturated with these elements.

The normalization of chemical elements to a natural marker allows for samples with different particle size distributions to be compared. Fe, as the

most suitable element for the Gdansk basin [*Uścinowicz et al.*, 2011], was selected as a normalizing agent. The accumulation of Fe is the result of natural processes and of the formation of various clay minerals which form silts (illite, kaolinite, chlorite, etc.). However, K, Na, Ca and Mg can additionally enter the upper part of the sedimentary sheath along with fluids. Normalization to a natural agent with a relatively uniform accumulation allows for such influxes to be identified in the sedimentary mass.

In general, above-limit normalized values of K, Na, Ca, and Mg to Fe for the fault area and background points replicated natural ratios (K – 23%, Na – 27%, Ca – 51%, Mg – 42%).

In the vertical distribution of normalized values, the increased values of K and Mg in Column 37056 at a depth of 25–40 cm, and of Mg and Ca in Column 37057, which may indicate endogenous introduction, deserve particular attention (Figure 2).

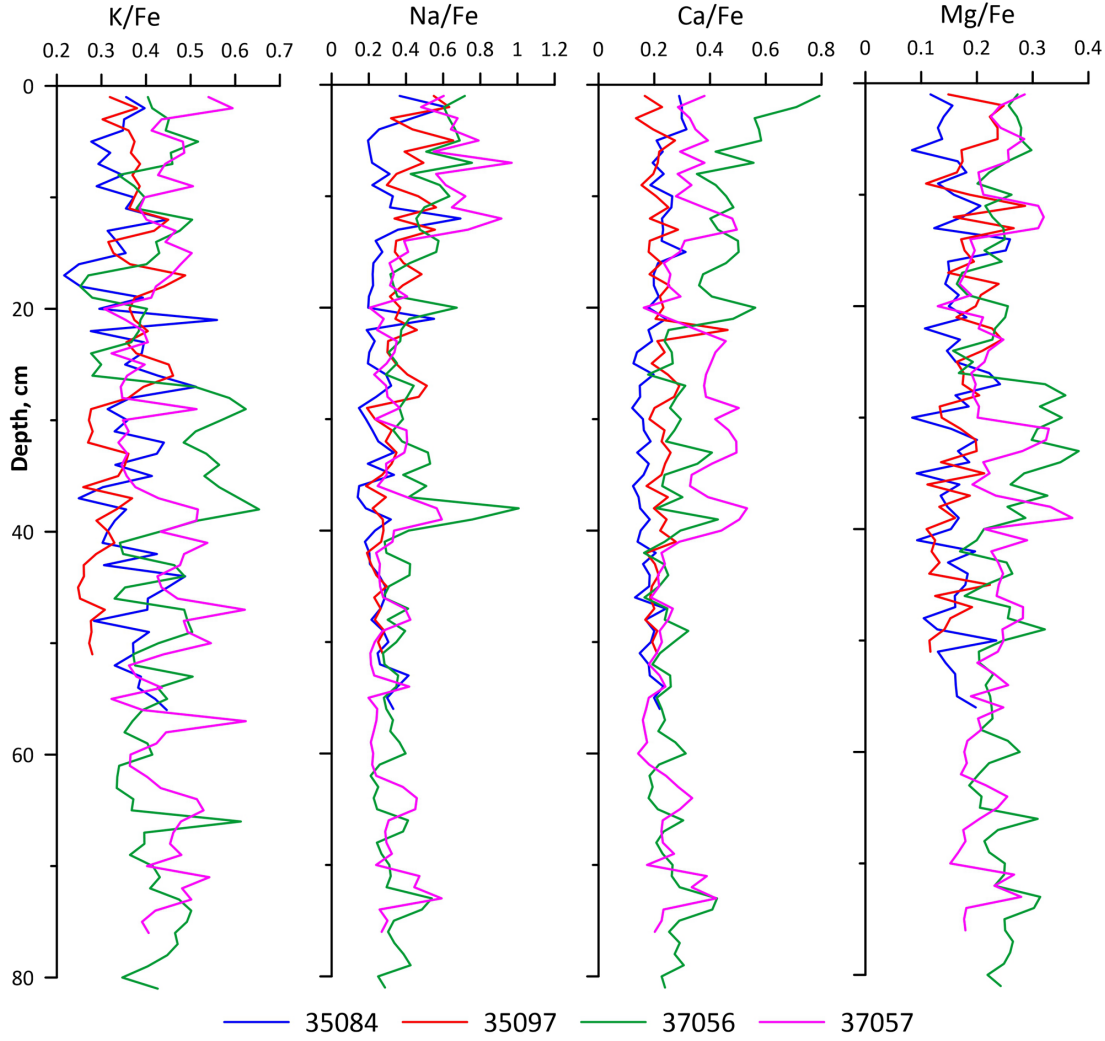


Figure 2. Vertical distribution of the ratios to Fe.

Discussion

Cluster Analysis of Columns by Layers

Based on the results of the cluster analysis, significant differences in the grouping of layers by cm were identified in the background and pockmark area columns.

Background Columns

The relationships between the layers distinguish several major groups in the background columns. The surface layer is group A (1–5 cm for Column 35097 and 1–4 cm for Column 35084, Fig-

ure 3), and the subsurface group is B, reflecting the interaction of the water column with interstitial water (6–28 cm for Column 35097 and 5–23 cm for Column 35084). Groups C and D make up the lower layers. Layers in Column 35084 are more compressed, probably due to a different sediment accumulation rate. Thus, its larger column length at a lower sediment accumulation rate allows Group D to be singled out.

Column 35084. Differentiation between the surface and lower layers occurs at a bond length of 39 units. Two groups are identified in close proximity to the surface: group A and group B are separated by a bond length of 20 units. Apparently, the current influence of bottom seawater becomes negligible at horizons deeper than 23 cm. The subsur-

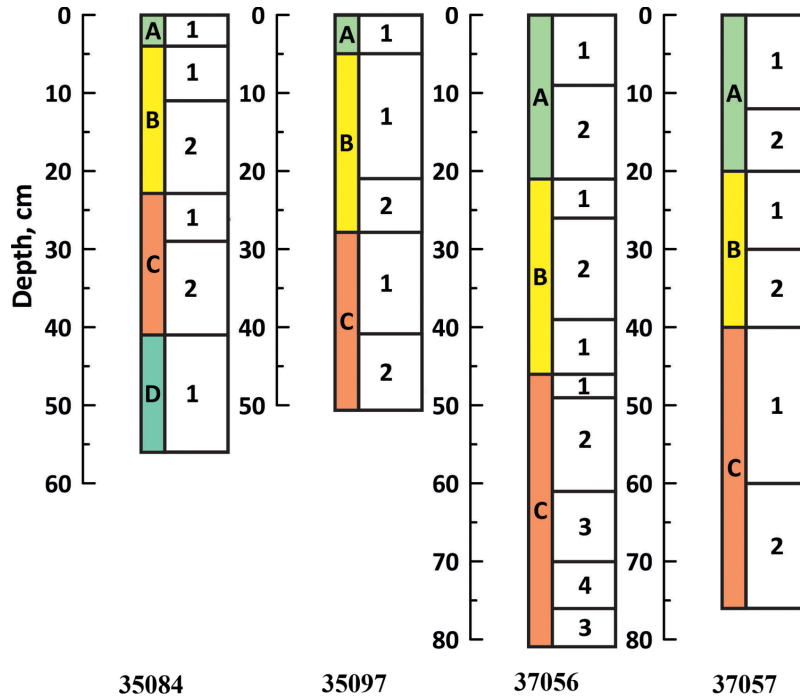


Figure 3. Grouping of layers in columns of bottom sediments based on the results of cluster analysis.

face group B has two subgroups with a bond length of about 12 units (B1 and B2). Groups C and D have a bond length of about 16 units. In group C, the length of bonds between layers C1 and C2 decreases slightly in comparison with group B, and amounts to 10 units. Layers in groups A, B, C and D are classified according to their occurrence (see Figure 3).

Column 35097. Differentiation between groups A and B occurs at a bond length of 22 units. Group C, with a bond length of 39 units, is distinguished separately. In this case, the current influence of bottom seawater does not extend deeper than to 28 cm. Two subgroups with a bond length of about 10 units are distinguished in the subsurface group B and group C (B1–B2 and C1–C2). Layers are classified according to their occurrence (see Figure 3).

Columns in the Fault Area

The thin subsurface layer in the fault area is not classified into a separate group, and it is represented by a lower rank. In the pockmark region, an inconsistent (alternating classification) occurrence

of layers by the distribution of elements has been identified.

Column 37056. With a bond length of 57 units, the surface layer is classified as a separate group A, with a thickness of 21 cm, which is divided into subgroups A1 and A2 by 22 units. Although it shows stratification, the consistent sediment occurrence in groups A1 and A2 is more blurred than in the background areas. The absence of a thin boundary surface layer in the background columns indicates, with a high degree of probability, the mixing of sediment by the flows of fluids.

Differentiation between groups B and C occurs at 34 units. In group B (bond length of 16 units), two subgroups B1 (12 units) and B2 (8 units) are distinguished. Layers of 22–26 cm and 40–46 cm fall into subgroup B1, and the intermediate layer of 27–39 cm falls into group B2. For the upper B1 layer, the bonds between marker elements do not exceed 4 units. For B2, they extend to 16 units, and, for the lower B1 layer, they shorten again to 5 units (Figure 4).

Interconnections are similarly distributed in group C (the length of bonds for the entire group is 18 units). Alternating horizons, with layers of 62–70 cm and 77–81 cm, belong to Subgroup C3 (see

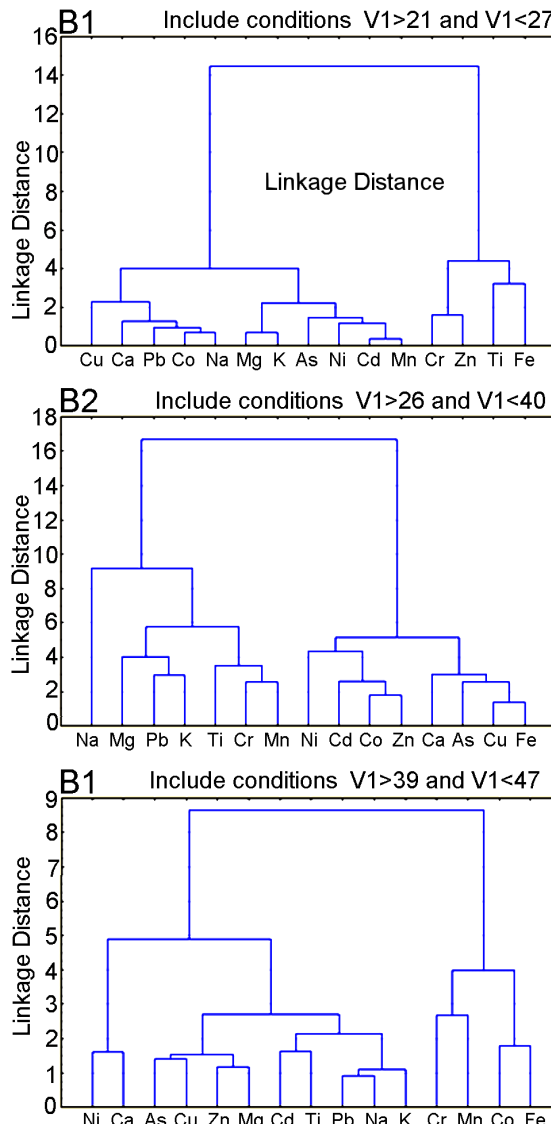


Figure 4. Cluster analysis by elements for layers B based on occurrence (see Figure 3).

Figure 3). In C3, the bonds between the marker elements are shortened to 6–7 units, with an average of 20 units for group C.

Such column inconsistency is suggestive of endogenous exposure, most likely due to fluid influx.

Column 37057. Differentiation between surface group A and groups B and C occurs at a bond length of 48 units. As with Column 37056, a thin surface layer, apparently blurred due to internal exposure, is not classified as a separate group. Group A, with a thickness of 20 cm, is divided by layers into subgroups A1 and A2 at a bond length of 20 units.

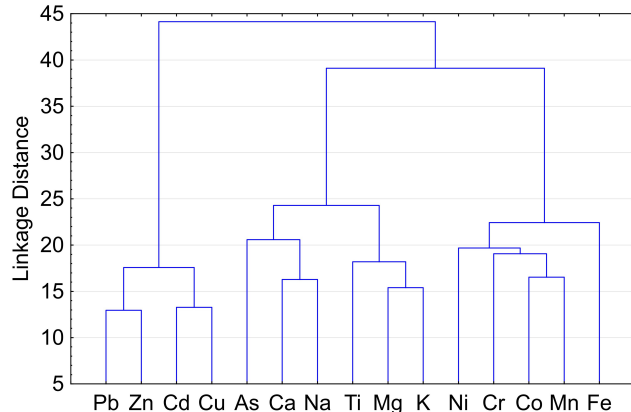


Figure 5. Results of cluster analysis of the entire data sample for the 0–22 cm layer.

Groups B (21–40 cm) and C (41–76 cm) are separated at 45 units. B1 and B2 are separated at 10 units and are represented by an ordered stratification of layers; the boundary between B1 and B2 is somewhat provisional. The length of the bonds between the marker elements in B1 and B2 is 13 and 15 units, respectively.

In group C, the division into C1 and C2 occurs at a value of 25 units. The length of the bonds between the layers in C1 and C2 does not exceed 10 units. With increase in depth, the marker elements undergo a shortening of bonds from 16 to 9 units (see Figure 3).

Column Analysis by Chemical Elements

In the statistical analysis of the entire sample of values (Columns 35097, 35094, 37056 and 37057), the group of elements of anthropogenic origin, including Pb, Zn, Cd, and Cu, appears to stand apart.

The accumulation of anthropogenic elements is of high statistical significance and is characteristic of the 0–22 cm layer (Figure 5). The formation of this layer coincides with the age of industrialization [Krek et al., 2019; Uścinowicz et al., 2011]. Strong anthropogenic interference with the environment has led to the establishment of clear relationships between Pb, Zn, Cd and Cu. Distribution of cluster groups in the upper layer replicated the distribution throughout the sample (along the entire length of the columns), indicating that the anthropogenic activity reflected in the surface layer of the sediment exceeded the intensity of natural pro-

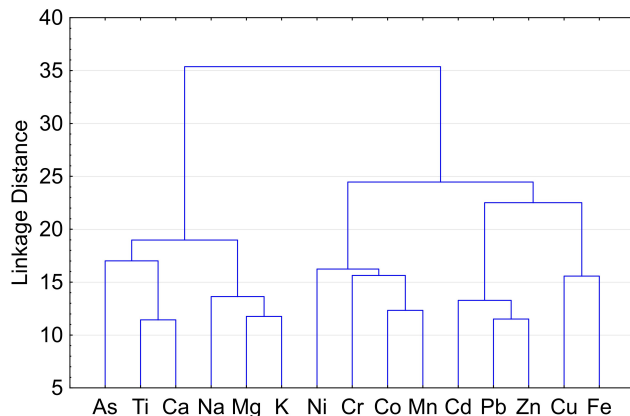


Figure 6. Cluster analysis of columns of the layer deeper than 22 cm.

cesses in the area studied. This is a very important issue for further studies of geochemical processes in silt sediments.

The distribution pattern of the elements is quite different below the 0–22 cm layer. The group of Pb, Zn, Cd and Cu is similar to Fe and Zn, which indicates their natural origin. Na, Mg, K have regular close bonds and are close to Ca, As, and Ti. Due to the absence of exposure to the surface, the bonds between Ca and Ti are shortened (Figure 6).

A clear relationship in the 22–84 cm layer between the group of the Na, Ca, Mg, and K marker elements with a bond length of 10 units (Figure 7) is a characteristic of fluid influx into Column 37056. In the remaining columns, this group is not observed and the bonds are more blurred.

The vertical structure and level of interconnections of chemical elements in Column 37056 allow us to assert the existence of additional factors affecting sedimentogenesis. Such dissimilarity with the adjacent Column 37057 cannot be explained by different sediment accumulation conditions. It is difficult to imagine the development of different hydrological and hydrochemical conditions which could determine the distinct mineralogical composition of the deposits on a scale of several kilometers under the halocline in the Gdansk Deep. The proximity of the pockmark to Column 37056 marks the egress of fluid from the sedimentary mass, which apparently created features of repeated stratification.

The principal sources of sediment matter in the Gdansk deep are coastal and submarine nearshore slope abrasion, which significantly exceeds river

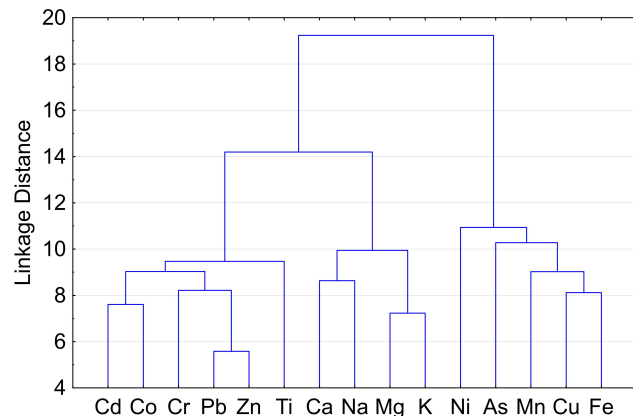


Figure 7. Grouping of elements based on the results of cluster analysis of Column 37056, 22–84 cm layer.

flow in terms of incoming material [Emelyanov, 1987].

The background columns are located at a considerable distance from Column 37056. However, they are similar by their sea depth and belong to the same sedimentation basin. The shift from reducing conditions to oxidizing in the deep-water part of the Gdansk Deep occurs during large inflows of North Sea waters, resulting in the movement of aerated water, which clings to the eastern slope of the deep. In such cases, the bottom layers of water mix, and the agitated sediment is transported by the generated bottom currents. In the vertical exchange of sedimentary material, the halocline (also known as the pycnocline) serves as a formidable barrier for fine suspension. Halocline and cyclonic circulation in the bottom layer prevents the creation of local anomalies in chemical composition during the influx of sedimentary material from above, along the slope. It is likely that the influx of minerals of terrigenous origin in the form of fine particles will cover significant areas, comparable to the area of the sedimentation basin. The localization of the anomaly of the high Na, Ca, Mg, and K content and its confinement to gas-saturated sediments suggests its endogenous origin.

Conclusion

Increased concentrations of Na, Ca, Mg and K have been identified as a result of the geochemical investigation of bottom sediment columns in the

area of tectonic faults of the Russian sector of the Gdansk Deep. The hydrologic regime of the near-bottom layer, sedimentation conditions in the basin under the pycnocline, tectonic faults and the known composition of artesian groundwater suggest that this anomaly is endogenous in origin. The closest bonds of the submarine discharge marker elements in the fault area were found at a depth of 22–84 cm. It appears to be obvious that the discharge occurs in a pulsed mode. The alternation of the B1–B2 and C3–C4 cluster layers in Column 37056 suggests the intermittent flow of fluids. Discharge is most pronounced in layers deeper than 20 cm – the mixing layer. Apparently, this layer is a marker layer, where the effect of submarine discharge changes the order of bonds between the elements and creates a geochemical anomaly due to the introduction of elements from the subsurface.

Acknowledgments. The reported study was funded by RFBR and Government of the Kaliningrad region according to the research project No. 19-45-390007. Bottom sediments sample collection was done with a support of the state assignment of IO RAS (Theme No. 0149-2019-0013).

References

- Blazhchishin, A. I. (1985), Lithostratigraphic Complexes of Deepwater Sediments, *Litho- and Biostratigraphy of Bottom Sediments of the Baltic Sea*, Gudelis V. K. (Ed.) p. 15–53, Mokslas, Vilnius. (in Russian)
- Blazhchishin, A. I. (1998), *Paleogeography and Evolution of the Late Quaternary Sedimentation in the Baltic Sea*, 160 pp. Yantarnyj Skaz, Kaliningrad. (in Russian)
- Bulczak, A. I., D. Rak, et al. (2016), Observations of near-bottom currents in bornholm basin, slupsk furrow and gdansk deep, *Deep Sea Research Part II: Topical Studies in Oceanography*, 128, 96–113, [Crossref](#)
- Burnett, W. C., P. K. Aggarwal, et al. (2006), Quantifying submarine groundwater discharge in the coastal zone via multiple methods, *Science of the total Environment*, 367, No. 2–3, 498–543, [Crossref](#)
- Charette, M. A., K. O. Buesseler, J. E. Andrews (2001), Utility of radium isotopes for evaluating the input and transport of groundwater-derived nitrogen to a Cape Cod estuary, *Limnology and Oceanography*, 46, No. 2, 465–470.
- Earth Physics Institute, RAS (2008), Comprehensive Seismological and Seismotectonic Studies for Assessment of the Seismic Hazard of the Kaliningrad Territory in 2008, Scientific and Technical Report, p. 306, O. Y. Schmidt Earth Physics Institute of the RAS, Moscow. (in Russian)
- Emelyanov, E. M. (1986), Suspension and Sediment Geochemistry in the Gdansk Basin and Sedimentation Processes, *Geochemistry of Sedimentary Process in the Baltic Sea* p. 57–114, Nauka, Moscow.
- Emelyanov, E. M. (1987), Distribution of Chemical Elements and components in Bottom Sediments and Particular Features of their Diagenesis, *Sedimentation Processes in the Gdansk Basin (Baltic Sea)*, E. M. Emelyanov, K. Vypykh (Eds.) p. 217–242, AN USSR, Moscow.
- Emelyanov, E. M. (1998), *Ocean Barrier Areas. Sedimentation and Ore Formation, Geoecology*, 416 pp. Yantarnyj Skaz, Kaliningrad.
- Emelyanov, E. M., (Ed.) (2002), *Geology of the Gdansk Basin. Baltic Sea*, 496 pp. Yantarnyj Skaz, Kaliningrad. (in Russian)
- Emelyanov, E. M. (2017), Bottom Sediments: Distribution, Particle Size Distribution, Mineralogy, Geochemistry, *Baltic Sea System* p. 380–474, Nauchny Mir, Moscow.
- Grigyalis, A. A., A. R. Kondratas, (Eds.) (1983), *State Geological Map of the USSR on a Scale of 1:200,000. Baltic Series. Sheet N-34-VIII, IX. Explanatory Note*, 116 pp. Northwest Territorial Geological Survey, Moscow. (in Russian)
- Khandros, G. S., Y. O. Shaidurov (1980), *Chemical Analysis of Marine Sediments*, 50 pp. Nauka, Moscow. (in Russian)
- Krek, A., A. Danchenkov, et al. (2019), Heavy metals contamination of the sediments of the south-eastern Baltic Sea: the impact of economic development, *Baltica*, 32, 1.
- Lund-Hansen, L. C., P. Skym (1992), Changes in hydrography and suspended particulate matter during a barotropic forced inflow, *Oceanologica Acta*, 15, No. 4, 339–346.
- Mohrholz, V., M. Naumann, et al. (2015), Fresh oxygen for the Baltic Sea – An exceptional saline inflow after a decade of stagnation, *Journal of Marine Systems*, 148, 152–166, [Crossref](#)
- Moore, W. S. (2010), The effect of submarine groundwater discharge on the ocean, *Annual Review of Marine Science*, 2, 59–88, [Crossref](#)
- Nikutina, N. G. (2011), Hydrogeology, *State Geological Map of the Russian Federation. Scale 1:1,000,000 (third generation). Central European Series. Sheet N-(34)-Kalinigrad. Explanatory Note: Lukyanova N. V., et al. p. 104–128*, VSEGEI Map-Making Factory, SPb..
- Oberdorfer, J. A., M. A. Valentino, S. V. Smith (1990), Groundwater contribution to the nutrient budget of Tomales Bay, California, *Biogeochemistry*, 10, No. 3, 199–216, [Crossref](#)
- Otmas, A. A., V. M. Desyatkov, et al. (2006), Tectonic Zoning of the Kaliningrad Region and the Adjacent Shelf, *Geology, Geophysics and Development of Oil and Gas Fields*, 8, 13–24.
- Pempkowiak, J., A. Sikora, E. Biernacka (1999),

- Speciation of heavy metals in marine sediments vs their bioaccumulation by mussels, *Chemosphere*, 39, No. 2, 313–321, [Crossref](#)
- Petrov, O. V., (Ed.) (2010), *Atlas of Geological and Environmental Geological Maps of the Russian Area of the Baltic Sea*, 78 pp. VSEGEI, SPb.. (in Russian)
- Roussiez, V., W. Ludwig, et al. (2005), Background levels of heavy metals in surficial sediments of the Gulf of Lions (NW Mediterranean): an approach based on ^{133}Cs normalization and lead isotope measurements, *Environmental Pollution*, 138, No. 1, 167–177, [Crossref](#)
- Rubio, B., M. A. Nombela, F. Vilas (2000), Geochemistry of major and trace elements in sediments of the Ria de Vigo (NW Spain): an assessment of metal pollution, *Marine Pollution Bulletin*, 40, No. 11, 968–980, [Crossref](#)
- Sidorenko, A. V., (Ed.) (1970), *Hydrogeology of the USSR: Volume XLV: Kaliningrad Region*, 158 pp. Nedra, Moscow. (in Russian)
- Slomp, C. P., P. Van Cappellen (2004), Nutrient inputs to the coastal ocean through submarine groundwater discharge: controls and potential impact, *Journal of Hydrology*, 295, No. 1–4, 64–86, [Crossref](#)
- Sviridov, N. I. (1990), Geological and Physical Nature of Geoacoustic Anomalies in the Upper Part of the Sedimentary Sheath of the Baltic Sea, *Geoacoustic and Gas-Lithogeochemical Studies in the Baltic Sea. Geological Features of Fluid Discharge Areas*, Geodekyan A. A., Trotsyuk V. Y., Blazhchishin A. I. (Eds.) p. 47–56, IO AN USSR, Moscow. (in Russian)
- Sviridov, N. I., E. M. Emelyanov (2000), Facial and Lithological Complexes of the Quaternary Deposits of the Central and South East Baltic, *Lithology and Minerals*, 3, 246–267, [Crossref](#)
- Szymczycza, B., K. D. Kroeger, J. Pempkowiak (2016), Significance of groundwater discharge along the coast of Poland as a source of dissolved metals to the southern Baltic Sea, *Marine Pollution Bulletin*, 109, No. 1, 151–162, [Crossref](#)
- Szymczycza, B., A. Maciejewska, et al. (2014), Could submarine groundwater discharge be a significant carbon source to the southern Baltic Sea?, *Oceanologia*, 56, No. 2, 327–347, [Crossref](#)
- Szymczycza, B., S. Vogler, J. Pempkowiak (2012), Nutrient fluxes via submarine groundwater discharge to the Bay of Puck, southern Baltic Sea, *Science of the Total Environment*, 438, 86–93, [Crossref](#)
- Triponis, A. I. (1973), Gas and Biochemical Anomalies of Underground Reservoirs in the Area of Intensive Water Exchange and their Relationship with Deep Oil and Gas Potential, In collection “*Issues of Oil and Gas Content in the Baltic states*”. Works of LitNIGRI. Issue 24 p. 169–184, Mintis, Vilnius.
- Ulyanova, M., V. Sivkov, et al. (2012), Methane fluxes in the southeastern Baltic Sea, *Geo-Marine Letters*, 32, No. 5–6, 535–544, [Crossref](#)
- Uścinowicz, Sz., P. Szefer, K. Sokołowski (2011), Trace Elements in the Baltic Sea Sediments, *Geochemistry of Baltic Sea surface sediments* p. 356, Polish Geological Institute – National Research Institute, Warsaw.
- Ward, J. H., Jr. (1963), Hierarchical grouping to optimize an objective function, *Journal of the American Statistical Association*, 58, No. 301, 236–244, [Crossref](#)
- Zagorodnykh, V. A. (2011), Neotectonics, *State Geological Map of the Russian Federation. Scale 1: 1,000,000 (third generation). Central European Series. Sheet N-(34)-Kalinigrad, Explanatory Note*. Lukyanova N. V. et al. (Eds.) p. 93–98, VSEGEI Map-Making Factory, SPb. (in Russian)

Corresponding author:

Alexander Krek, P. P. Shirshov Institute of Oceanology – Atlantic Branch, 1 Prospect Mira, 236022 Kaliningrad, Russia. (av_krek_ne@mail.ru)